Tellus (1996), 48A, 733–749
Printed in UK – all rights reserved

Copyright © Munksgaard, 1996
TELLUS
ISSN 0280–6495

A comparison of two strategies on land surface heterogeneity used in a mesoscale β meteorological model

By NICOLE MÖLDERS*, ARMIN RAABE AND GERD TETZLAFF, *LIM Institut für Meteorologie, Universität Leipzig, Stephanstraße 3, D-04103 Leipzig, Germany*

(Manuscript received 12 October 1995; in final form 26 January 1996)

ABSTRACT

Results of case studies with a mesoscale β meteorological model applying two different strategies to treat subgrid-scale surface heterogeneity are compared with each other to evaluate the effects of these strategies on the predicted hydrologically relevant quantities. In the first strategy, the mosaic approach, different land-use types are considered as separate patches within a grid cell independently interacting with mean atmospheric field quantities of that grid cell. Feedback to the grid scale is accomplished by forming area-weighted quantities from the fluxes provided by the individual patches for the soil-biosphere-atmosphere interaction. In the second strategy, a higher resolution subgrid is established within each model grid cell and the soil-biosphere-atmosphere interaction is determined for each subgrid cell with its individual soil and biosphere conditions and near-surface meteorological forcing. Probability density functions are used to evaluate the statistical behavior of both the strategies. It is substantiated that the partitioning of the atmospheric radiative and moisture forcing at the surface as well as cloud and precipitation formation can significantly be affected by the type of strategy. Using the explicit subgrid strategy results in a shift in the partitioning of energy towards decreasing Bowen ratios as compared to the mosaic approach. For very heterogeneous surfaces with strongly varying soil types and plant species an area-weighted meteorological near-surface forcing as used in the mosaic approach may artificially reduce evapotranspiration. An explicit subgrid strategy or individual near-surface meteorological forcing within the mosaic approach seems to be more adequate under such surface conditions.

1. Introduction

Estimates of the impact of the Earth's surface properties on cloud and precipitation formation, evapotranspiration as well as on runoff require information on spatial scales far smaller than those explicitly resolved by the grid cells of atmospheric models. Obviously, for these purposes the exchange of water and energy fluxes at the interface Earth-atmosphere cannot be treated with the assumption that the fluxes occurring within each grid cell are represented by those of its dominant land-use type. Hence, several different strategies have recently been developed to parameterize subgrid-scale surface heterogeneity, for instance, by averaging surface properties (Lhomme, 1992; Dolman, 1992), or by statistical-dynamical approaches (Wetzel and Chang, 1988; Entekhabi and Eagleson, 1989). Computationally more expensive procedures to consider patchy surface properties are the mosaic approach (Avissar and Pielke, 1989), the explicit subgrid strategy (Seth et al., 1994), or the mixture strategy, wherein for the different surface types tightly coupled energy balances are determined (Sellers et al., 1986; Dickinson et al., 1986; Kramm et al., 1994). Several authors comparing the results provided by simulations with and without consideration of subgrid-scale surface heterogeneity found that for very patchy surfaces large differences in the predicted

fluxes can occur (Avissar and Pielke, 1989; Seth et al. 1994; Mölders and Raabe, 1996). By comparing the mixture and the mosaic approach, Koster and Suarez (1992) found that the effective differences between these two strategies are small over a wide range of conditions. Using data of 3 field experiments Mahrt and Sun (1996) concluded that assuming spatially constant atmospheric variables and spatially varying surface conditions closely approximates the area composite fluxes. Note that detailed reviews of strategies to consider subgrid-scale heterogeneity are given by Mahrt and Sun (1995) and Mölders and Raabe (1996).

Obviously, such strategies are especially required within the framework of GEWEX, and its related regional projects like BALTEX, GAME, GCIP, LAMBADA, and MAGS for coupling meteorological and hydrological models to simulate the water cycle in a straight-forward manner. A key research activity within this context is to develop strategies to downscale meteorological quantities for the application in hydrological models (which on their part have to be upscaled).

Hence, for modeling a closed water cycle, concepts to include subgrid-scale surface heterogeneity have to be tested and evaluated with respect to their suitability to deliver those meteorological input data as requested by hydrological models. If it is necessary, these strategies have to be further developed for the purpose mentioned above.

In a first step, the results obtained by two different strategies to consider subgrid-scale heterogeneity, namely the 'mosaic approach' (Avissar and Pielke, 1989) and the 'explicit subgrid strategy' (Seth et al., 1994), are compared with each other with respect to the goals of BALTEX. The focus is on these strategies because the mosaic approach is often used in hydrological modeling to deal with subgrid-scale processes. Furthermore, the explicit subgrid strategy on its part seems to be easily compatible to hydrological models like MIKE SHE (Refsgaard et al., 1992).

In the mosaic approach each grid cell area is divided into homogeneous subregions (denoted as patches) according to the different land-use types occurring within that grid cell (Fig. 1). Assuming that horizontal fluxes between the different patches within a grid cell are small in comparison to the corresponding vertical transfer processes, these patches of the same land-use type are rearranged into a single patch, for which the energy and water fluxes, soil temperatures and soil wetness are once calculated no matter where the individual patches are located within the grid cell (Fig. 1). Hence, no advective effects accompanied with occasionally observed internal boundary layers (IBL; Raabe, 1983; 1991; Garratt, 1992; Hupfer and Raabe, 1994) as well as no subgrid-scale dynamical effects related to land surface heterogeneity like directed flows caused by topography are considered. Mean grid cell atmospheric field quantities (in the immediate vicinity of the surface and at reference height) as well as the individual soil wetness and soil temperatures serve for the calculations of the energy and water fluxes. Feedback to the grid scale is accomplished by forming area-weighted fluxes describing the exchange between the soil-biosphere system and the atmosphere. The advantage of this approach is (1) that an arbitrary number of land-use types can be added without complication of the energy balance calculation and (2) that this approach is computationally efficient. Besides the deficiencies mentioned before a further disadvantage is that the location where within the grid cell the fluxes occur is more or less unknown (Fig. 1).

In the second strategy, a higher resolution grid consisting of several subgrid cells is defined for each grid cell (Fig. 1). These subgrid cells are considered to be homogeneously covered by their individual vegetation and soil types. For each subgrid cell unique energy and hydrological budgets are maintained using the subgrid cell forcing at the representative location, i.e., the fluxes in each subgrid cell are calculated with their own subgrid soil temperatures, soil wetness and near-surface meteorological forcing in the immediate vicinity of the Earth's surface. A fundamental assumption of this strategy is that the subgrid-scale near-surface meteorological forcing, which is experienced by the surface, is important in determining the net exchange of heat, moisture and momentum at the interface Earth-atmosphere. Like in the mosaic approach, however, no interaction between the different land-use types exists. The advantage of the subgrid strategy is that by explicitly breaking down the grid cells of the atmospheric model the spatial location of each subgrid flux is known (Fig. 1). Its disadvantage is that it is computationally expensive.

Numerical experiments were carried out using a mesoscale β meteorological model, where the

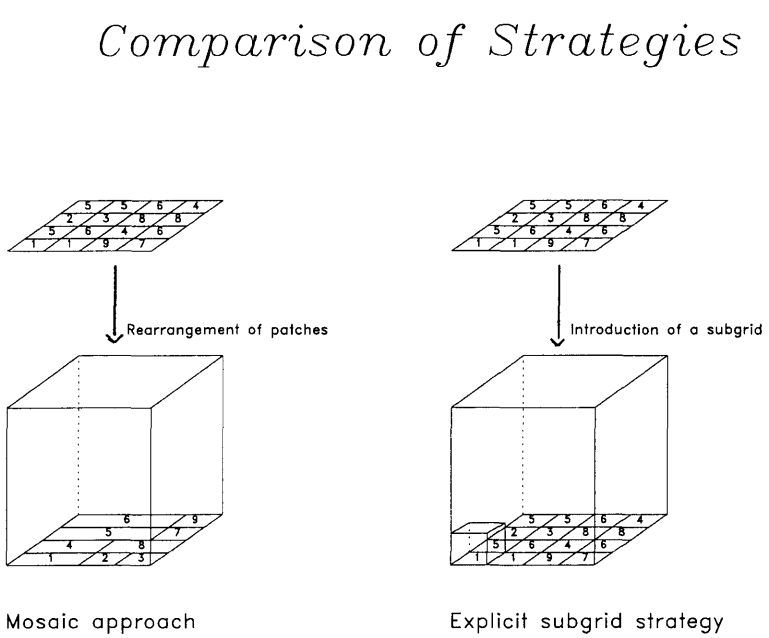

Fig. 1. Schematic plot of an atmospheric grid cell at the boundary Earth-atmosphere exemplary showing how the land-use types within a grid cell are rearranged in the mosaic approach (left) and how the explicit subgrid is introduced in the explicit subgrid strategy (right) for the land-use types within an atmospheric grid cell. The upper parts show the land-use types as given for the respective atmospheric grid cell by the land-use data set and the numbers indicate different land-use types as given in Fig. 2, Table 1. In the explicit subgrid strategy the small box represents a subgrid cell. See text for further explanation.

same surface exchange and turbulence parameterization schemes are embedded into the strategies mentioned above to ensure that differences in the results are only affected by these different strategies. Following Entekhabi and Brubaker (1995) the differences in the land-atmosphere interaction caused by these two strategies are evaluated on the basis of probability density functions of the model state variables, the water and energy fluxes as well as the cloud and precipitating particles.

2. Description of the strategies

In both the strategies the energy equation, $Q+L_vE+H=G$, is calculated in accord with Eppel et al. (1995) but using the formulations of the fluxes as required by the respective strategy. Note that in the case of the water bodies (land-use types 1 to 3 in Table 1) the energy budget is always closed by the residuum of net radiation and the fluxes of sensible and latent heat.

2.1. Mosaic approach

In the mosaic approach, mean grid cell atmospheric field quantities as well as individual soil wetness and soil temperatures serve to calculate the energy and water fluxes of the different land-use types within a grid cell. Hence, the net radiation, Q, the soil heat flux, G, as well as the fluxes of latent, L_vE, and sensible heat, H, of the ith land-use type in the jth grid cell are given by

$$Q_{i,j} = -S_j(1-\alpha_{i,j}) - \varepsilon_{i,j}L_j + \varepsilon_{i,j}\sigma T_{sj}^4 , \quad (1)$$

$$G_{i,j} = -\lambda_{i,j}\partial T_{si,j}/\partial z , \quad (2)$$

$$L_vE_{i,j} = \rho L_v C_{qi,j} u_{Rj} (q_{sj}(T_{sj}) - q_{Rj}) w_{ei,j} , \quad (3)$$

$$H_{i,j} = \rho c_p C_{hi,j} u_{Rj} (\Theta_{sj} - \Theta_{Rj}) , \quad (4)$$

where Θ and q represent the potential temperature and specific humidity at the surface (index s) and the reference height (index R) located at the first half level of the model in this study, i.e., in 10 m height above ground. Furthermore, α, ε, λ, σ, S and L stand for the albedo, the emissivity of the

Table 1. *Soil and plant parameters as used in the model*

	Land-use type	k_s 10^{-6} m^2/s	c_i 10^6 $J/m^3/K$	ε	α	z_0 m	θ_{sf} m	α_c 10^{-3} $kg/m^3/s$	g_1 m/s	$T_{W/s}$ K
1	water deeper than 10 m	0.14	4.2	0.95	*	*	1	1000	0	277
2	water less than 10 m deep	0.14	4.2	0.95	*	*	1	1000	0	279
3	lake/river	0.15	4.2	0.94	*	*	1	1000	0	283
4	sand	0.84	2.1	0.90	0.3	0.0004	0.002	0.9	0	*
5	grassland	0.56	2.1	0.95	0.25	0.07	0.01	8	0.04	*
6	agriculture	0.84	2.1	0.95	0.25	0.17	0.003	1	0.04	*
7	heather/bushland	0.7	2.5	0.95	0.15	0.35	0.003	1	0.024	*
8	deciduous forest	0.7	2.5	0.97	0.28	0.8	0.01	8	0.023	*
9	mixed forest	0.7	2.5	0.95	0.25	0.75	0.01	8	0.023	*
10	coniferous forest	0.7	2.5	0.98	0.23	1.	0.01	8	0.023	*
11	village	1	2	0.90	0.2	0.8	0.003	1	0	*
12	town	1	2	0.95	0.15	1	0.002	0.9	0	*

With reference to Deardorff (1978), Oke (1978), Pielke (1984), Wilson et al. (1987), and Eppel et al. (1995): Temperature diffusivity, k_s, heat capacity, c_i, (note that $\lambda = k_s c_i$) emissivity, ε, albedo, α, roughness length, z_0, field capacity, θ_{sf}, capillarity, α_c, maximal evaporative conductivity, g_1, and water and ground surface temperature, $T_{W/s}$. The quantities indicated by * are calculated by the model. Note that the water surface temperatures are held constant throughout the entire simulations.

surface, the soil thermal conductivity, the Stephan-Boltzmann constant, the shortwave and longwave radiation, respectively. T_s is the surface temperature, and u_R is the wind speed at the reference height. The density of air is denoted as ρ, c_p and L_v are the specific heat at constant pressure and the latent heat of condensation, C_h and C_q are the transfer coefficients for heat and water vapor. For bare soil the so-called wetness factor, w_e, equals the soil surface wetness while for vegetated surfaces it considers the canopy conductivity, g_s, which depends on the maximal evaporative conductivity, g_1 (Table 1), the insolation, the water vapor deficit, the air temperature and the soil wetness (Deardorff, 1978)

$$w_{ei,j} = g_{si,j}/(g_{si,j} + C_{qi,j} u_{Rj}). \quad (5)$$

Area-weighted fluxes, F_j^k, for the interaction of the soil-biosphere-atmosphere system for the jth grid cell are given by (Avissar and Pielke, 1989)

$$F_j^k = \sum_{i=1}^{n} a_{i,j} F_{i,j}^k, \quad (6)$$

where $F_{i,j}^k$ is the particular flux provided by the ith subgrid land-use type in the jth grid cell and $a_{i,j}$ is the relative area of the subgrid-scale land-use type i. The exponent k indicates the different fluxes (H, L_vE, G, Q) and n is the number of land-use types occurring in the jth grid cell. Note that in our study n varies between 1 and 12 (Table 1) depending on how much land-use types occur in the jth grid cell. The area-weighted values of humidity and temperature at the surface, soil temperatures and soil wetness are obtained similarly. Note that Mölders and Raabe (1996) used area-weighted means of the soil wetness, surface and soil temperatures in eqs. (2) and (3) which leads to slightly less evapotranspiration than that achieved with our formulation.

2.2. *Explicit subgrid strategy*

In contrast to the mosaic approach, in the explicit subgrid strategy the near-surface meteorological as well as the soil forcing are individually calculated and stored for each subgrid cell. A homogeneous land-use type is assumed for each subgrid cell. The fluxes for the mth subgrid cell of the jth grid cell are, therefore, written as

$$Q_{m,j} = -S_{m,j}(1-\alpha_{m,j}) - \varepsilon_{m,j} L_{m,j} + \varepsilon_{m,j} \sigma T_{sm,j}^4, \quad (7)$$

$$G_{m,j} = -\lambda_{m,j} \partial T_{sm,j}/\partial z, \quad (8)$$

$$L_v E_{m,j} = \rho L_v C_{qm,j} u_{Rj} (q_{sm,j}(T_{sm,j}) - q_{Rj}) w_{em,j}, \quad (9)$$

$$H_{m,j} = \rho c_p C_{hm,j} u_{Rj} (\Theta_{sm,j} - \Theta_{Rj}), \quad (10)$$

with

$$w_{em,j} = g_{sm,j}/(g_{sm,j} + C_{qm,j} u_{R,j}). \quad (11)$$

The grid cell fluxes, F_j^k, of the jth grid cell are represented by the arithmetic means

$$F_j^k = \frac{1}{N^2} \sum_{m=1}^{N^2} F_{m,j}^k , \tag{12}$$

determined from the individual fluxes, $F_{m,j}^k$, within its subgrid cells, and N^2 (=16 in our study) is the number of subgrid cells occurring within that jth grid cell. In contrast to the mosaic approach, in the explicit subgrid strategy the heterogeneity of precipitation, $P_{m,j}$, is considered by

$$P_{m,j} = (z_{m,j}/z_j)\, P_j , \tag{13}$$

where z_j and $z_{m,j}$ are the mean terrain height of the jth grid cell and the mth subgrid cell and P_j is the mean precipitation predicted for the jth grid cell.

3. Model description

The Leipzig's mesoscale model version of the non-hydrostatic meteorological model GESIMA (**GE**esthacht's **SI**mulation **M**odel of the **A**tmosphere; Kapitza and Eppel, 1992; Eppel et al., 1995) is used in our study. Its dynamical part is based on the anelastic equations. An improved version of Jacob's (1991) bulk-parameterization for cloud microphysics is applied considering condensation and deposition of water vapor, rainwater formation by autoconversion and coalescence, accretion of cloud water by ice, homogeneous freezing of cloud water and rainwater, evaporation of cloud water and rainwater, melting, sublimation, as well as sedimentation of rainwater and ice. A saturation adjustment scheme assuming mass-weighted saturation mixing ratios and a temperature dependent partitioning of the excess water vapor between condensation and deposition rates (Lord et al., 1984; Mölders et al., 1995) is used. The parameterization of the soil-vegetation-atmosphere interaction follows Deardorff (1978; see also Eppel et al., 1995). The surface stress and the near-surface fluxes of heat and water vapor are expressed in terms of dimensionless drag and transfer coefficients according to eqs. (3), (4), (9) and (10) using the parametric model of Kramm et al. (1995) which is based on the Monin-Obukhov similarity theory. Above the atmospheric surface layer the turbulent fluxes of momentum are calculated by a one-and-a-half-order closure scheme according to level 2.5 in the hierarchy of Mellor and Yamanda (1974). Here, the elements of the eddy diffusivity tensor are expressed by the vertical eddy diffusivity, $K_{M,V}$, and the horizontal eddy diffusivity, $K_{M,H}$, where the latter is also related to $K_{M,V}$ by the simple linear relationship $K_{M,H} = 2.3\ K_{M,V}$. Furthermore, $K_{M,V}$ is expressed by the turbulent kinetic energy (TKE) and the mixing length, l, using the Kolmogorov-Prandtl relation where the mixing length is parameterized by Blackadar's (1962) approach slightly modified by Mellor and Yamanda (1974). The turbulent fluxes of sensible heat and water vapor are expressed as functions of $K_{M,V}$ and the turbulent Prandtl number, $Pr_t = K_{M,V}/K_{H,V}$, and the turbulent Schmidt number, $Sc_t = K_{M,V}/K_{E,V}$, respectively. These characteristic numbers are considered to be functions of the thermal stratification. They were derived from the local stability functions of Businger et al. (1971) and the assumption that $Sc_t = Pr_t$. To determine the TKE, an additional budget equation for that quantity is solved, where the energy production due to horizontal shear is neglected (for more detail, see Kapitza and Eppel (1992)). Note that the parametric model for the atmospheric surface layer (Kramm et al., 1995) agrees with the turbulence parameterization scheme used for the model domain above that layer. Radiation transfer is calculated by a simplified two stream method (Eppel et al., 1995). Modified versions of the mosaic approach proposed by Avissar and Pielke (1989) and of the explicit subgrid strategy recommended by Seth et al. (1994) were implemented into the Leipzig's mesoscale model version to consider subgrid-scale surface heterogeneity.

4. Experimental design

4.1. Model domain

The model domain encompasses the troposphere over the mouth of the river Elbe and parts of the western Baltic Sea from the surface to a height of 11.5 km with a horizontal extension of (the inner grid of) 128 km in the North-South and 200 km in the West-East direction (Fig. 2). This inner grid domain is surrounded by five grid points (outer grid), which are treated with the strategy of dominant land-use types to ensure equal and homogeneous inflow and outflow condi-

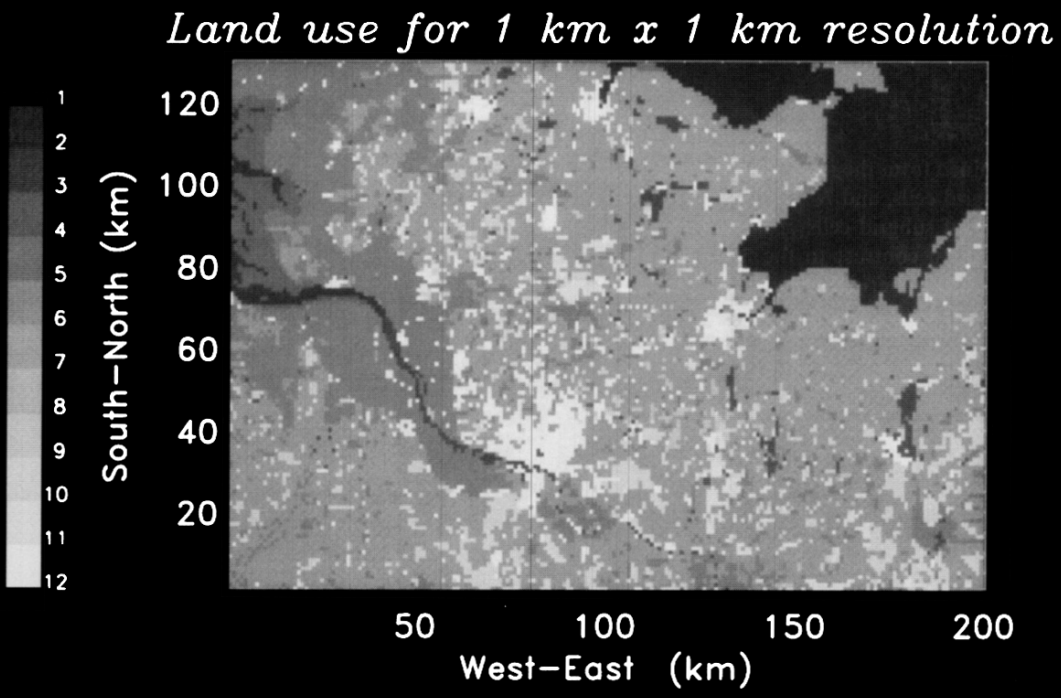

Fig. 2. Land-use data set for the inner model domain with a 1×1 km^2 resolution (after Mölders and Raabe, 1996). The numbers represent the land-use types as follows: 1 water deeper than 10 m, 2 water less than 10 m deep, 3 lake/river, 4 sand, 5 grassland, 6 agriculture, 7 heather/bushland, 8 deciduous forest, 9 mixed forest, 10 coniferous forest, 11 village, and 12 town.

tions, whatever strategy to treat subgrid-scale surface heterogeneity is utilized.

The model region is characterized by relatively flat topography, strongly eroded heterogeneous soils, shallow water tables, water meadows, bogs, small lakes and settlements. For simplicity, in our study the soil type is connected with the land-use type (Table 1) to avoid additional degrees of freedom (e.g., if *agriculture* occurs once with a soil which nearly holds its moisture and once with a rapidly drying soil).

The horizontal grid resolution applied is 4×4 km^2 and the vertical resolution varies from 20 m close to the ground to 1 km at the upper model domain with 8 levels below 2 km and 7 levels above that height. A time step of 10 s is used to fulfill the Courant-criterion.

4.2. *Initialization*

The 3D-simulations were initialized with the same profiles of wind, moisture, air and soil temperature obtained from a 1D-simulation (Fig. 3), which adjusts the vertical profiles of temperature and wind speed to homogeneous terrain. These profiles are orientated at the synoptic situation of 26 April, 1986. Soil wetness and soil temperature in 1 m depth were set equal to 0.02 and 280 K, respectively.

4.3. *Modeling strategy*

Two numerical experiments were performed alternatively applying the mosaic approach and the explicit subgrid strategy. All other aspects of the model were kept the same so that the results isolate the sensitivity of hydrologically relevant quantities to the treatment of subgrid-scale surface heterogeneity. The available land-use data set has a resolution of 1×1 km^2 (Fig. 2) and distinguishes 12 land-use types for which different plant and soil parameters are considered (Table 1). To ensure that the same surface composition is applied in both runs the resolution of the subgrid was chosen

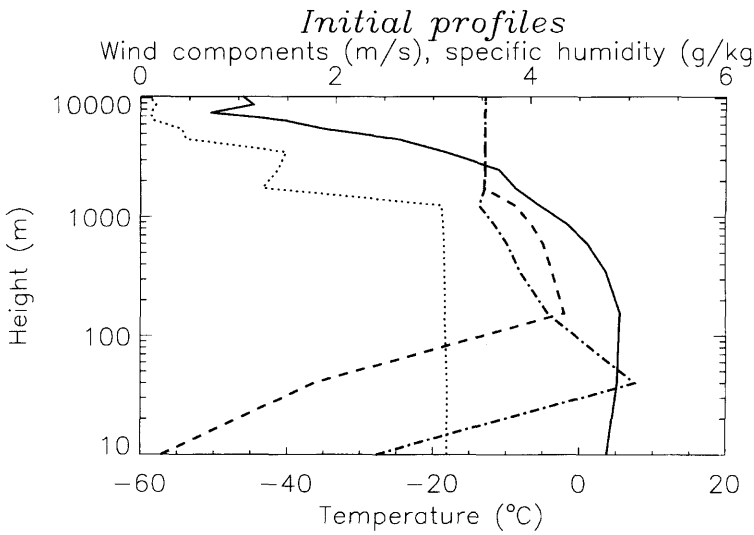

Fig. 3. Initial profiles of temperature (solid line), moisture (dotted), u (dashed) and v (dash-dotted) components of the horizontal wind vector.

to be 1×1 km^2. If, for instance, two subgrid cells of 1 km^2 are covered by *sand* in the explicit subgrid strategy, 2 km^2 (12.5 %) of the 16 km^2 grid cell are covered by *sand* in the mosaic approach, too (see also Fig. 1).

To ensure the same terrain height conditions for both runs, a mean terrain height within each grid cell is assumed. Note that in the region under study the land-use type does not depend on the terrain height. Such a dependence could occur, for instance, in mountainous regions like the Scandinavian Ridge or the Rocky Mountains because of the tree line, the orographic snow line, etc..

Obviously, the obtained results may only differ by effects attributed to the different treatment of surface forcing, i.e., area-weighted averaged atmospheric and individual soil conditions in the mosaic approach versus individually near-surface meteorological and soil forcing for each subgrid cell in the explicit subgrid strategy, respectively.

5. Results

The results provided by the simulations with the mosaic approach and the explicit subgrid strategy are addressed hereafter as MA4 and SUB4, respectively. The temperature and moisture states in the system Earth-atmosphere evolve by fluxes which themselves depend on those states. The resultant non-linear dynamical system has modes of variability and statistical signatures that depend on the interactions of the energy and water budget (Entekhabi and Brubaker, 1995). To evaluate the statistical behavior of the effects of the strategies, frequency distributions of the model state quantities, the water and energy fluxes as well as the cloud and precipitating particles were determined for the entire simulation time on the basis of the hourly data provided for the inner grid by the two runs. The probability density function of a quantity is given by (e.g., Olberg and Rakóczi, 1984)

$$\mathrm{pdf}(\chi) = p(\chi \leqslant X \leqslant \chi + \Delta X)/\Delta X, \tag{14}$$

where p is the frequency in the interval $(\chi, \chi + \Delta X)$.

Since there are complex non-linear interactions and feedback processes between the variables of states, the water and energy fluxes as well as cloud and precipitation formation, which are evaluated in Subsections 5.1 to 5.4, the discussion of the results is started with an overall evaluation of the simulations. Sometimes it is unavoidable that a certain aspect is presented before its occurrence is explained.

Generally, the differences in all quantities predicted by the two simulations are larger during the daytime than during the nighttime due to the

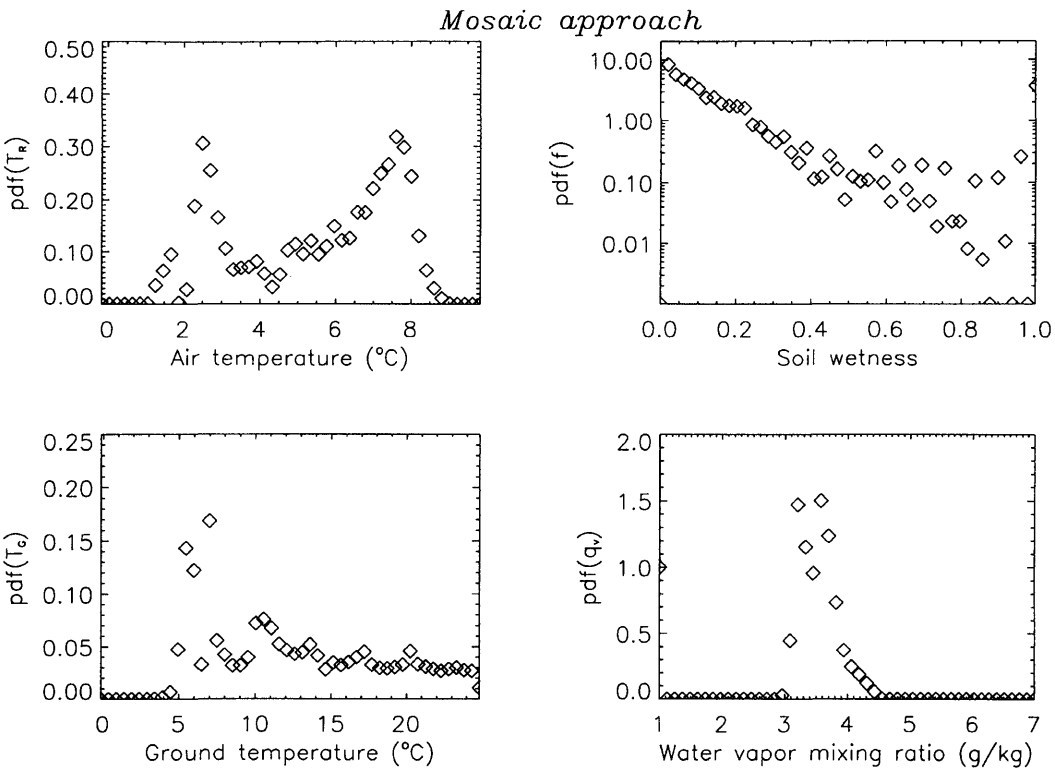

Fig. 4. Probability density functions, pdf, from upper left to lower right corner for air temperatures, T_R, at reference height (in 10 m), soil wetness factor, f, ground temperatures, T_G, and water vapor, q_v, at reference height for the simulation using the mosaic approach.

strong interrelation between the atmospheric water cycle and the energy budget. However, in the mid and upper troposphere the predicted temperature, moisture, and cloud distributions are only hardly affected by the strategy applied to consider subgrid-scale surface heterogeneity. Somewhat larger differences occur in cloudy regions resulting from differences in phase transition processes, vertical motions, turbulence or radiative cooling.

Compared with the mid and upper troposphere, the impact of both the strategies to consider the subgrid-scale surface heterogeneity on the predicted air temperatures and moisture is larger in the atmospheric boundary layer (ABL). Here, the differences in water vapor and temperature increase when approaching the Earth's surface. In the ABL the cloud fields obtained by SUB4 are smoother and more extended than those of MA4. Moreover, the cloud bases predicted by SUB4 occur in lower levels than those obtained by MA4.

5.1. *Variables of state*

Figs. 4, 5 show the probability density functions as calculated by the two runs for the air temperature and water vapor at reference height, soil wetness and ground temperature. Compared to MA4 (Fig. 4) the probability is skewed towards cooler surface and air temperatures as well as towards larger moisture and soil wetness in SUB4 (Fig. 5), i.e., the ABL and the soil are drier and warmer for the former than for the latter. Discrepancies in the predicted water vapor mixing ratios of up to 0.0015 kg/kg and in the air temperatures of up to 2.5 K locally occur. The key point leading to these differences (and those in steps of them) is that the soil and the near-surface meteoro-

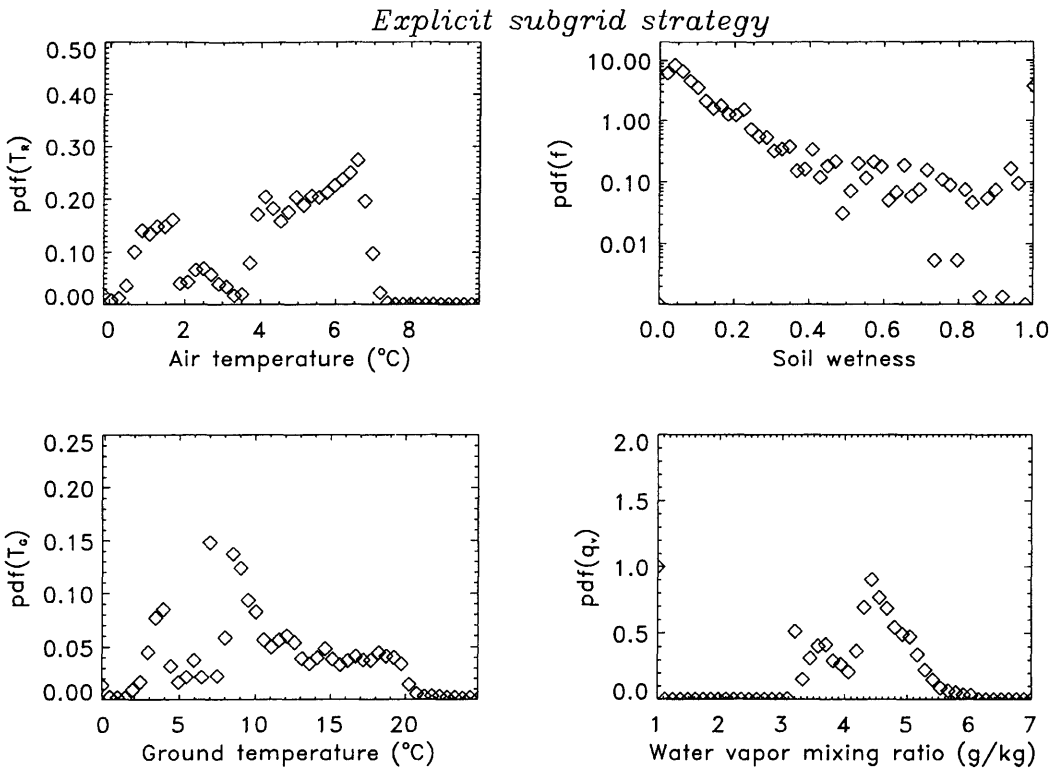

Fig. 5. As Fig. 4 but for the simulation with the explicit subgrid strategy.

logical forcing is treated differently. Effectively, area-weighted contributions to the change in humidity and temperature at the Earth's surface are considered in the mosaic approach while in the explicit subgrid strategy the different subgrid cells maintain their own meteorological conditions at the Earth's surface.

In MA4 the use of area-weighted near-surface meteorological conditions to calculate the near-surface fluxes smoothes the contrasts between the various land-use types. This may lead to a more stable stratification of the ABL for MA4 than for SUB4. Seemingly, the grid cell area-weighted averages of the predicted meteorological quantities at the Earth's surface and the area-weighted fluxes (see eq. (6)) result in a simultaneous and partially compensating underestimation of the soil moisture and overestimation of the vapor deficit above wetter areas of the grid cell. Similar, but working in the opposite direction, is true for the drier patches of the grid cell. Note that such a mechanism was already found by Shuttleworth (1988). The area-weighted near-surface meteorological forcing means that during the daytime the usually cool and moist environment of a *forest*, for instance, may be suppressed by the near-surface microclimate of other land-use types within a grid cell having a warmer and/or drier near-surface microclimate. The area-weighted near-surface atmospheric conditions may pretend for the warmer/drier surfaces of the grid cell a relatively cooler/moister atmosphere as compared to the atmosphere which would be in 'equilibrium' with that land-use type. On the contrary, for the cooler/moister areas the area-weighted near-surface atmospheric conditions delude a relatively warmer/drier atmosphere as compared to their 'equilibrium' atmosphere. Consequently, in the former case evapotranspiration is reduced. Whereas, in the latter case it is enhanced. This mechanism also contributes to the larger probabilities for drier soils in MA4 than in SUB4.

The mechanism mentioned above is one reason for the differences in soil wetness. Another reason

(but not so important in this case study) is that occasionally slight amounts of precipitation were predicted by both the runs. The horizontal pattern of this slight precipitation and the intensity are slightly larger for SUB4 than for MA4, for which soil wetness increases less and at less locations for the former than for the latter. The precipitation pattern may also differ due to the fact that a homogeneous precipitation distribution is assumed within a grid cell in MA4 while non-uniform precipitation is realized in SUB4.

As illustrated in Figs. 4, 5, MA4 provides a larger probability for warmer surface temperatures (up to 2.5 K) than SUB4. The sequence of several small maxima and minima in the distributions reflects the more frequently occurring land-use types within a grid cell (e.g., *agriculture*, *water*, *grassland*). The curve of the probability functions is smoother for MA4 than for SUB4. This arises from the use of area-weighted near-surface meteorological forcing used in the former strategy. The large probabilities for surface temperatures around 5°C, 7°C and 10°C are due to grid cells fully or partly covered by water. Low probability, for instance, occurs for surface temperatures larger than 20°C. Such surface temperatures are achieved during the daytime for grid cells which are more or less dominated by conurbation.

During the daytime the larger cloudiness obtained from SUB4 reduces insolation and results in lower surface temperatures and less warming of the ABL in SUB4 than in MA4. The stronger evaporative cooling caused by the larger evapotranspiration in SUB4 than in MA4 also leads to lower air temperatures in the ABL at daytime. During the nighttime the larger cloudiness of SUB4 reduces the longwave radiation into space. Hence, the air temperatures hardly fall below those of MA4 during the nighttime. Altogether, the effects discussed above skew the probability of the air temperatures at reference height towards larger values for MA4 as compared to SUB4 (Figs. 4 and 5).

5.2. *Water and energy fluxes*

Even though the surface exchange and the turbulence parameterization schemes are the same in both the strategies, discrepancies in these processes occur caused in the steps of the different strategies. The use of a mean wind vector for the entire grid cell as applied in both the strategies means that effects on the velocity and direction of the wind by directed flows or IBLs are not included. Of course, such effects may differently influence the fluxes calculated for the different patches or subgrid cells and demand further research.

Generally, the subgrid-scale heterogeneity simultaneously affects the water and energy fluxes. The atmospheric energy and water cycles are coupled by the evapotranspiration and the respective latent heat flux. The key role of the land surface energy budget is the partitioning of available energy between the latent and sensible heat fluxes which may be characterized by the Bowen ratio, $B=H/L_vE$. It is well established that the surface energy and water exchange and, hence, evapotranspiration are controlled by site-specific properties (e.g., roughness length, emissivity, albedo, soil specific parameters) and time dependent quantities (e.g., solar radiation, wind speed, soil temperature and soil moisture). Due to our modeling strategy, differences may only result from these time varying quantities, except for the roughness length over water (see Table 1).

The joint probability density function calculated for the results of MA4 are skewed to larger sensible and lower latent heat fluxes as compared to SUB4 (Figs. 6, 7). The reasons are manifold. As mentioned before, the soils are drier for MA4 than for SUB4. Dry soils are associated with larger Bowen ratios. Usually, rising air temperatures lead to an increase in potential evapotranspiration. However, in both the simulations the potential evapotranspiration is not achieved and the actual evapotranspiration is even lower for MA4 than for SUB4.

In contrast to MA4, in SUB4 precipitation may inhomogeneously be distributed within the area represented by an atmospheric grid cell. Generally, the consequence of precipitation events, of course, is a change in local energy partition leading to lower Bowen ratios, i.e., less sensible, more latent heat fluxes, which again alters the soil moisture and may induce cloud and precipitation formation. As pointed out already, in our case study only slight precipitation occurred at a few locations. Thus, the differences in soil wetness resulting from the heterogenization of precipitation in SUB4 remain small.

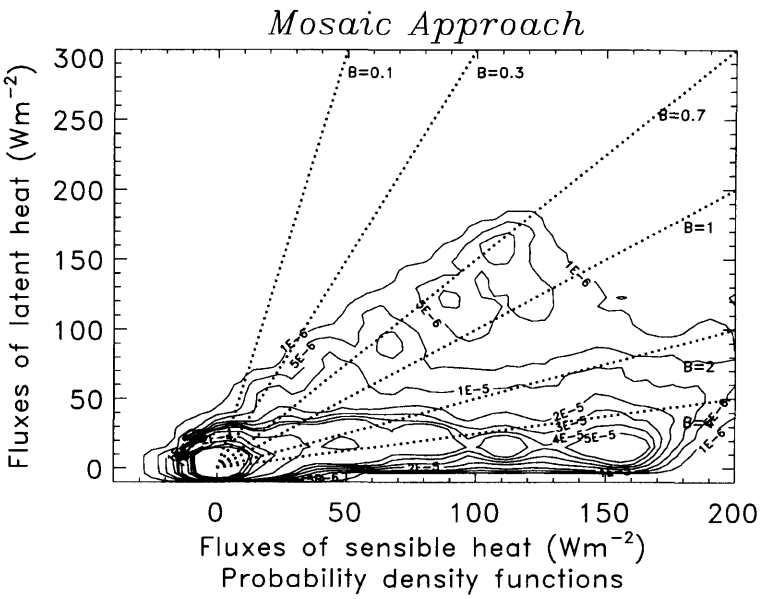

Fig. 6. Isolines of joint probability density functions for the surface fluxes of latent and sensible heat in the simulation using the mosaic approach. Lines of constant Bowen ratios are superimposed.

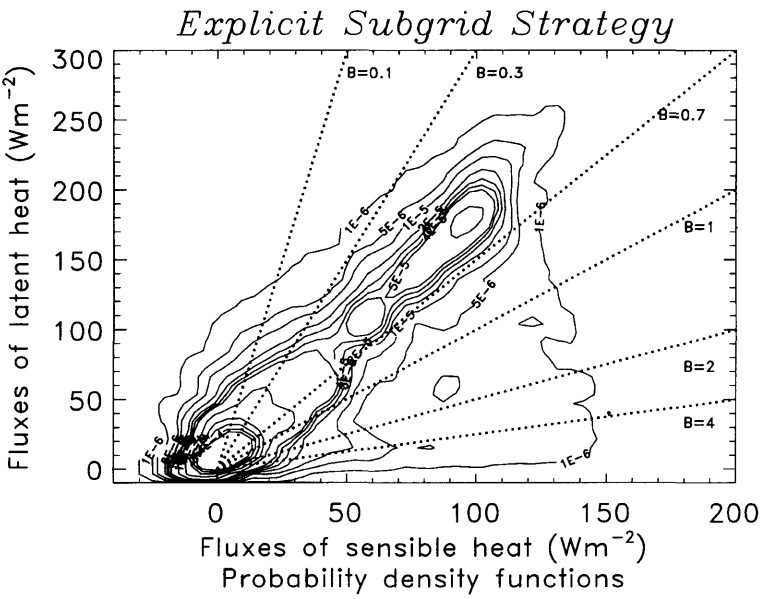

Fig. 7. As Fig. 6 but for the simulation with the explicit subgrid strategy.

Similar to the probability density functions of the surface temperatures the sequence of several maxima and minima in the distributions of the probability density functions of the latent and sensible heat fluxes is caused by the land-use types with large fractional coverage within the model domain. Again this distribution is smoother in MA4 than in SUB4 and the area-weighted near-

surface meteorological forcing yields to this smoothing effect.

On the average, the radiative flux is less sensitive to the treatment of subgrid-scale surface heterogeneity than to differences in cloudiness. For instance, the predicted distributions of net radiation (which are quite similar in cloudless regions) differ up to 50 Wm^{-2} and more in cloudy regions. These discrepancies in the predicted energy on their turn again conduce to differences in latent, sensible and soil heat fluxes. Since in MA4 the insolation is larger due to the lower cloudiness, the surface heats stronger than in SUB4 leading to slightly larger soil heat fluxes during the daytime for MA4 than for SUB4 (Figs. 8, 9). The latent heat flux and, hence, evapotranspiration is the most sensitive to the treatment of subgrid-scale surface heterogeneity.

5.3. Water in the atmosphere

The probability density functions of water vapor were determined for the whole model troposphere (Figs. 10, 11) and for the reference height (Figs. 4, 5). Those of the mixing ratios of cloud water, rainwater and ice were calculated for cloudy areas only (Figs. 10, 11). Note that the steps in the distribution for lower values of moisture are caused by the coarse discretization of the model in the upper troposphere. In this range the probabilities slightly differ due to small discrepancies in radiative cooling, vertical motions, turbulence as well as phase transition processes.

Since the atmosphere is moister (Figs. 4, 5, 10, 11) and colder (Figs. 4, 5) in SUB4 than in MA4, more clouds are predicted by the former rather than by the latter, i.e., there is a lower probability

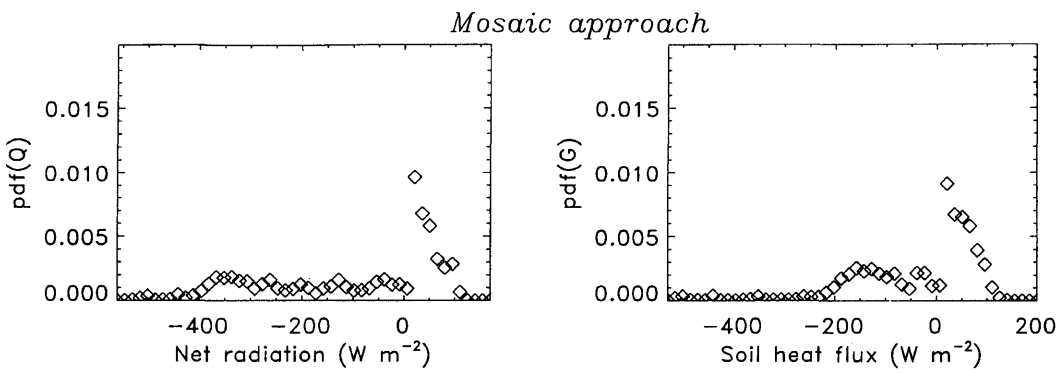

Fig. 8. As Fig. 4 but for net radiation (left) and soil heat flux (right) in the simulation using the mosaic approach.

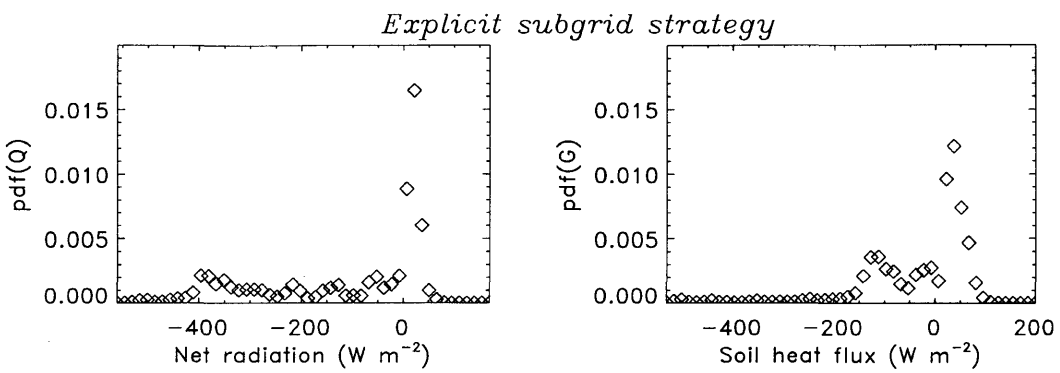

Fig. 9. As Fig. 8 but for the simulation with the explicit subgrid strategy.

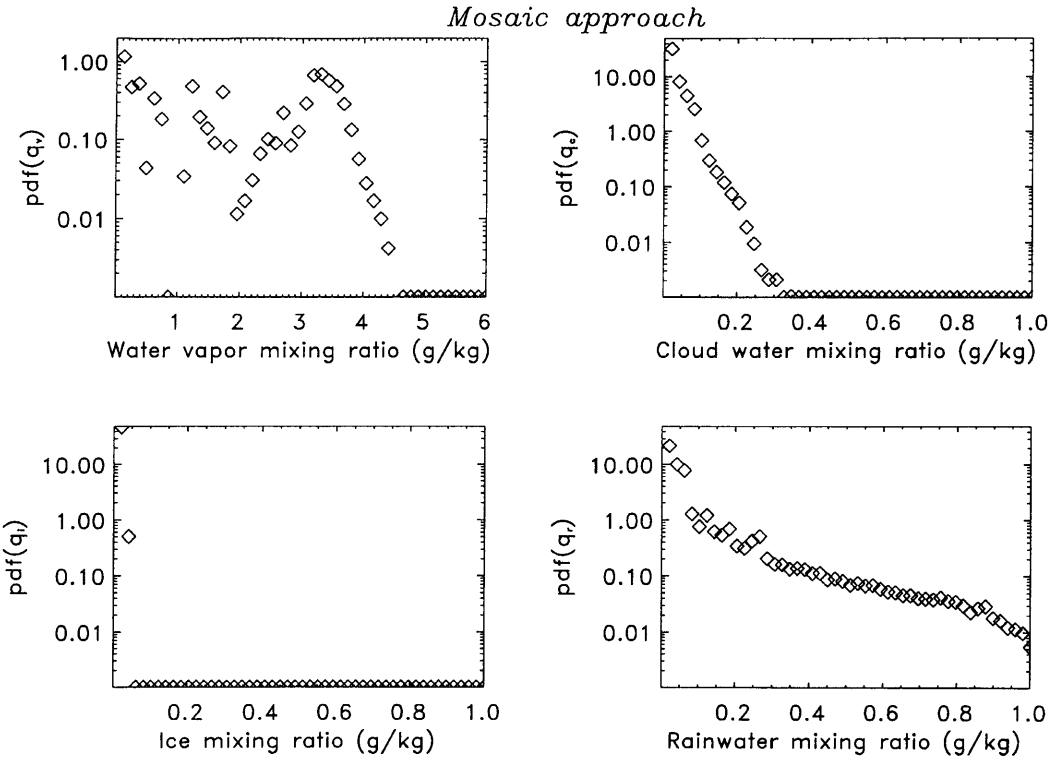

Fig. 10. As Fig. 4 but for the mixing ratios of water vapor, q_v, of the entire model atmosphere and of cloud water, q_c, ice, q_i, and rainwater, q_r, (from upper left to lower right) as obtained from the simulation using the mosaic approach.

for cloudless conditions in SUB4 than in MA4. Slightly larger probability exists for larger mixing ratios of rainwater and cloud water in SUB4 than in MA4, too (Figs. 10, 11).

The larger availability of water and the lower air temperatures contribute in several ways to the much larger ice formation and, hence, larger amount of ice in SUB4 than in MA4. The formulation of mass-weighted saturation mixing ratios in combination with temperature dependent condensation and water vapor deposition rates (Mölders et al., 1995), as applied in our study, leads to a shift towards an increasing formation of ice with decreasing temperature. Furthermore, ice passing the level of freezing survives longer distances at temperatures warmer than 0°C in SUB4 than in MA4 because the amounts of ice, which are to be melted, are larger in the former than in the latter strategies. Moreover, the lower water vapor mixing ratios in MA4 than in SUB4 also contribute to more sublimation of ice falling in subsaturated regions in MA4 than in SUB4. Therefore, the probabilities for ice mixing ratios below 0.0001 kg/kg increase for MA4 as compared to SUB4, whereas the probability is skewed towards larger ice mixing ratios for SUB4.

The horizontal extension of the rainwater fields and the values of the rainwater mixing ratios predicted by SUB4 are larger than those obtained by MA4. The latter is also manifested in larger probabilities for larger rainwater mixing ratios in SUB4 than in MA4 (Figs. 10, 11). The reasons are manifold. Since more ice is predicted in SUB4 than in MA4, more ice is available for rainwater formation by melting when the ice falls in regions warmer than 0° C. Furthermore, as the model atmosphere is moister and cooler in

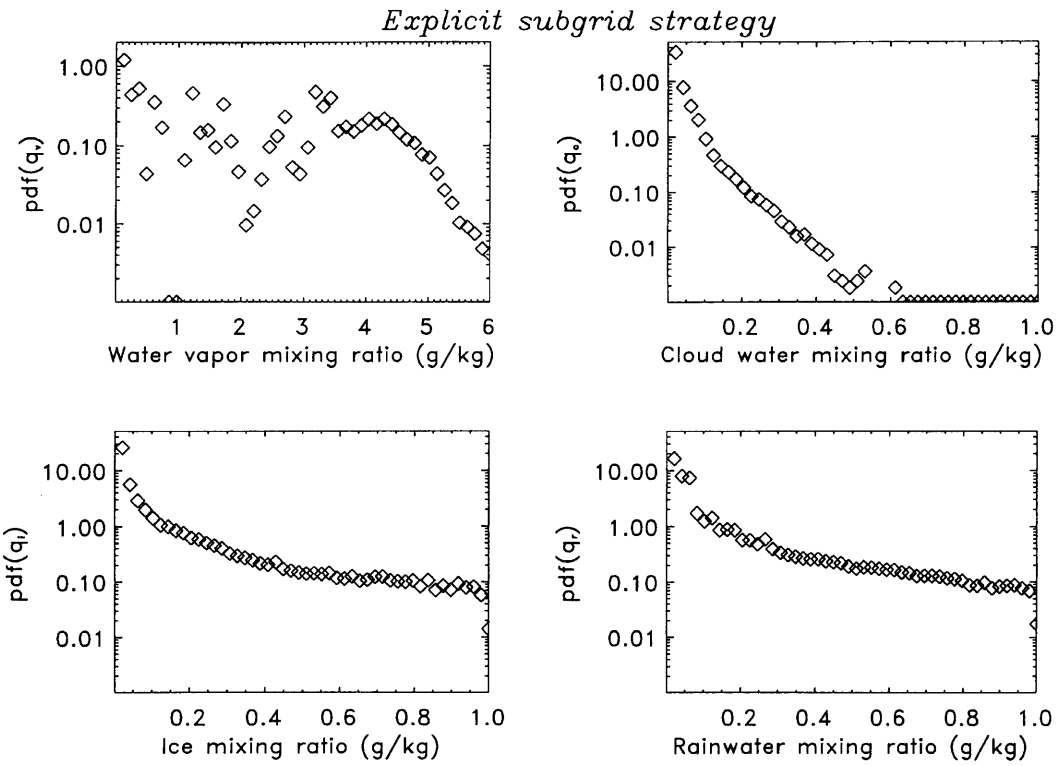

Fig. 11. As Fig. 10 but for the simulation with the explicit subgrid strategy.

SUB4 than in MA4, less rainwater evaporates in SUB4.

5.4. General feedback processes

In MA4 a feedback towards low soil wetness, low evapotranspiration, low cloudiness, stronger insolation and increased surface temperatures is established. On the contrary, in SUB4 the coupling reaches from wetter soils over larger evapotranspiration, specific humidity, cloud and precipitation formation to less insolation and lower surface and air temperatures as compared to MA4. The negative feedback between the decrease of evapotranspiration due to the increased cloudiness (which occurs in SUB4) seems to be less intensive than the positive feedback (established in MA4) where a dry soil state and low evapotranspiration contribute to their persistence.

As already pointed out, the feedback between evapotranspiration, cloud and precipitation formation is controlled by soil wetness, soil type, surface and soil temperature as well as near-surface meteorological conditions. Unfortunately, soil type, soil wetness and soil temperature are not well known because well appropriate data bases and initial data for the latter two quantities do not exist. In addition, problems arise from the large variability of virtually all soil specific properties. These points may also contribute to erroneous forecasts of precipitation as well as evapotranspiration and, hence, runoff. Therefore, sensitivity studies are planned to investigate (1) under which soil conditions, soil wetness or surface temperature gain the dominance in a certain feedback process and (2) the relative magnitudes of the feedback processes established.

6. Summary and conclusions

Numerical investigations were performed with a mesoscale β meteorological model using two different strategies to consider subgrid-scale sur-

face heterogeneity, namely a mosaic approach and an explicit subgrid strategy. The feedback and interactions found between evapotranspiration, soil wetness, cloud and precipitation formation (depending on the heat and moisture state of the soil and the near-surface atmosphere) are appreciably affected by those strategies. The key point leading to differences is the different treatment of the subgrid-scale surface meteorological forcing as well as the heterogeneity of precipitation which is only considered in the explicit subgrid strategy. The study affirms that the hydrologically relevant quantities like precipitation, evapotranspiration, and soil wetness may significantly be affected by these differences. Using the explicit subgrid strategy results in a shift in the partitioning of energy towards decreasing Bowen ratios as compared to the mosaic approach.

The advantage of the mosaic approach is (1) that an arbitrary number of land-use types can be added without complication of the energy balance calculation and (2) that this approach is computationally efficient. Its disadvantage is (1) that the location where within the grid cell the fluxes occur is more or less unknown and (2) that a heterogenization of precipitation cannot simply be realized. Besides of our results, the mosaic approach seems to be useful in cases where the size of the atmospheric grid cells approaches that of the hydrological grid cells, which is possible for regions without complicated hydrology and catchment basins.

The advantage of the explicit subgrid strategy is that the spatial location of each subgrid grid flux is well known. This means that the atmospheric model can be run on a far coarser grid than the hydrological model for which the water fluxes may be provided by a subgrid with the resolution required by the hydrological model. This, however, is accompanied with the main disadvantage of the explicit subgrid strategy that it is computationally expensive.

Based on our findings we conclude that the mosaic approach using area-weighted meteorological near-surface forcing may be overloaded for very heterogeneous surface conditions with strongly varying soil and vegetation types like established in our test region because the area-weighted near-surface meteorological conditions may tend to reduce evapotranspiration artificially. Although computationally more expensive, an explicit subgrid strategy, or individual near-surface meteorological forcing within the mosaic approach seems to be more adequate for applications in hydrological-meteorological modeling.

Of course, neither scheme should not be applied at scales much smaller than performed in our study, because the assumptions made on the parameterizations of the drag and transfer coefficients, for instance, are scale-dependent (Mahrt and Sun, 1995). Evaluation of the mosaic approach and the explicit subgrid strategy as well as of other representations of subgrid-scale surface heterogeneity by means of measured data must be postponed until complete suitable data sets are available. Here, the uncertainty in the measured data must be at least an order of magnitude lower than the differences between the simulations. This task will hopefully be addressed within the framework of the BALTEX field campaigns.

7. Acknowledgments

This study is funded by the Minister of education, science, research and technology (BMBF) of Germany within the framework of the water cycle project contract 521–4007–07 VWK 01. F. Jagusch provided the land-use and topography data for which we would like to express our thanks. The authors wish to thank Dr. G. Kramm from the Fraunhofer Institut für Atmosphärische Umweltforschung at Garmisch-Partenkirchen and the two anonymous reviewers for fruitful discussions.

8. List of symbols

$a_{i,j}$	relative area of the subgrid-scale land-use type i, -.-
c_i	heat capacity, J/m^3/K
c_p	specific heat at constant pressure, J/kg/K
g_1	maximal evaporative conductivity, m/s
g_s	canopy conductance, m/s
k_s	temperature diffusivity, m^2/s
l	mixing length, m
n	number of land-use types, -.-
q	specific humidity, kg/kg
u_R	wind at the reference height, m/s
w_e	wetness factor, -.-
z_o	roughness length, m

C_h	transfer coefficients for heat (index h), -.-
C_q	transfer coefficients for water vapor (index q), -.-
F_j^k	area-weighted fluxes for the jth grid cell, kg/s^3
$F_{i,j}^k$	flux of the ith land-use type in the jth grid cell, kg/s^3
$F_{m,j}^k$	flux in the mth subgrid cell of the jth grid cell, kg/s^3
G	soil heat flux, kg/s^3
H	sensible heat flux, kg/s^3
$K_{M,H}$	horizontal eddy diffusivity for momentum, m^2/s
$K_{M,H}$	vertical eddy diffusivity for momentum, m^2/s
$K_{H,V}$	vertical eddy diffusivity for heat, m^2/s
$K_{E,V}$	horizontal eddy diffusivity for moisture, m^2/s
L	longwave radiation flux, kg/s^3
L_v	latent heat of condensation, J/kg
L_vE	latent heat flux, kg/s^3
N^2	amount of subgrid cells within a grid cell, -.-
P	precipitation rate, kg/m^2/s
Pr_t	turbulent Prandtl number, -.-
Q	net radiation flux, kg/s^3
S	shortwave radiation, kg/s^3
Sc_t	turbulent Schmidt number, -.-
T_s	surface/soil temperature, K
T_W	water surface temperature, K
α	albedo, -.-
α_c	capillarity, kg/m^3/s
ε	emissivity of the surface, -.-
λ	soil thermal conductivity, J/K/m/s
ρ	density of air, kg/m^3
σ	Stephan-Boltzmann constant, kg/s^3/K^4
Θ	potential temperature, K
θ_{sf}	field capacity, m

References

Avissar, R. and Pielke, R. A. 1989. A parameterization of heterogeneous land surface for atmospheric numerical models and its impact on regional meteorology. *Mon. Wea. Rev.* **117**, 2113–2136.

Businger, J. A., Wyngaard, J. C., Izumi, Y. and Bradley, E. F. 1971. Flux profile relationship in the atmospheric surface layer. *J. Atmos. Sci.* **28**, 181–189.

Blackadar, A. K. 1962. The vertical distribution of wind and turbulent exchange in a neutral atmosphere. *J. Geophys. Res.* **67**, 3095–3103.

Chen, F. and Avissar, R. 1994. Impact of land-surface variability on local shallow convective cumulus and precipitation in large-scale models. *J. Appl. Met.* **33**, 1382–1401.

Deardorff, J. W. 1978. Efficient prediction of ground surface temperature and moisture, with inclusion of a layer of vegetation. *J. Geophys. Res.* **84C**, 1889–1903.

Dickinson, R. E., Henderson-Sellers, A., Kennedy, P. J. and Wilson, M. F. 1986. Biosphere-atmosphere transfer scheme (BATS) for the NCAR community climate model. *NCAR Technical Note 275+STR.*

Dolman, A. 1992. A note on areally-averaged evaporation and the value of the effective surface conductance. *J. Hydrol.* **138**, 583–589.

Entekhabi, D. and Brubaker, K. L. 1995. An analytical approach to modeling land-atmosphere interaction. 2. Stochastic formulation. *Water Resource Res.* **31**, 633–643.

Entekhabi, D. and Eagleson, P. 1989. Land surface hydrology parameterization for atmospheric general circulation models including subgrid-scale spatial variability. *J. Clim.* **2**, 816–831.

Eppel, D. P., Kapitza, H., Claussen, M., Jacob, D., Koch, W., Levkov, L., Mengelkamp, H.-T. and Werrmann, N. 1995. The non-hydrostatic mesoscale model GESIMA. Part II: Parameterizations and applications. *Contrib. Atmos. Phys.* **68**, 15–41.

Garratt, J. R. 1992. The internal boundary layer—a review. *Boundary Layer Meteorol.* **50**, 171–203.

Hupfer, P. and Raabe, A. 1994. Meteorological transition between land and sea in the microscale. *Meteorol. Zeitsch.* **44**, 100–103.

Jacob, D. 1991. Numerische Simulation der Wolkenbildung in einer Land-Seewind-Zirkulation. *GKSS Report 91/E/40* (in German).

Kapitza, H. and Eppel, D. P. 1992. The non-hydrostatic mesoscale model GESIMA. Part I: Dynamical equations and tests. *Contr. Phys. Atmos.* **65**, 129–146.

Koster, R. D. and Suarez, M. J. 1992. A comparative analysis of two land surface heterogeneity representations. *J. Clim.* **5**, 1379–1390.

Kramm, G., Dlugi, R., Mölders, N. and Müller, H. 1994. Numerical investigations of the dry deposition of reactive trace gases. In: J.M. Baldasano et al. (eds.) *Computer simulation air pollution II*, vol. 1, Computational Mechanics Publications, Southhampton Boston, 285–307.

Kramm, G., Dlugi, R., Dollard, G. J., Foken, T., Mölders, N., Müller, H., Seiler, W. and Sievering, H. 1995. On the dry deposition of ozone and reactive nitrogen compounds. *Atmos. Environ.* **29**, 3209–3231.

Lhomme, J.-P. 1992. Energy balance of heterogeneous terrain: averaging the controlling parameters. *Agri. For. Meteorol.* **61**, 11–21.

Lord, S. J, Willoughby, H. E. and Piotrowicz, J. M. 1984. Role of parameterized ice-phase microphysics in an

axisymmetric, nonhydrostatic tropical cyclone model. *J. Atmos. Sci.* **41**, 2836–2848.

Mahrt, L. and Sun, J. 1995. Dependence of exchange coefficients on averaging scale and grid size. *Q. J. Roy. Met. Soc.* **121**, 1835–1852.

Mellor, G. L. and Yamanda, T. 1974. A hierarchy of turbulence closure models for planetary boundary layers. *J. Atmos. Sci.* **31**, 1791–1806.

Mölders, N. and Raabe, A. 1996. Numerical investigations on the influence of subgrid-scale surface heterogeneity on evapotranspiration and cloud processes. *J. Appl. Meteor*, **35**, 782–795.

Mölders, N., Laube, M. and Kramm, G. 1995. On the parameterization of ice microphysics in a mesoscale α weather forecast model. *Atmos. Res.* **38**, 207–235.

Olberg, M. and Rakoczi, F. 1984. *Informationstheorie in der Meteorologie und Geophysik.* Akademie Verlag, Berlin.

Oke, T. R. 1978. *Boundary layer climates.* Routledge, London/New York.

Pielke, R. A. 1984. *Mesoscale meteorological modeling*, Academic Press, Inc., London.

Raabe, A. 1983. On the relation between the drag coefficient and fetch above the sea in the case of off shore wind in the near-shore zone. *Z. Meteor.* **6**, 363–367.

Raabe, A. 1991. Die Höhe der internen Grenzschicht. *Z. Meteor.* **41**, 251–261, (in German).

Refsgaard, J. C., Seth, S. M., Bathurst, J. C., Ehrlich, M., Storm, B., Jørgensen, G.H. and Chandra, S. 1992. Application of SHE to catchment in India—Part 1: General results. *J. Hydrol.* **140**, 1–23.

Sellers, P. J., Mintz, Y., Sud, Y. C. and Dalcher, A. 1986. A simple biosphere atmosphere model (SiB) for use within general circulation models. *J. Atmos. Sci.* **43**, 505–531.

Seth, A., Giorgi, F. and Dickinson, R. E. 1994. Simulating fluxes from heterogeneous land surfaces: explicit subgrid method employing the biosphere-atmosphere transfer scheme (BATS). *J. Geophys. Res.* **99** D9, 18651–18667.

Shuttleworth, W. J. 1988. Macrohydrology—the new challenge for process hydrology. *J. Hydrol.* **100**, 31–56.

Wetzel, P .J. and Chang, J.-T. 1988. Evapotranspiration from nonuniform surfaces: A first approach for short-term numerical weather prediction. *Mon. Wea. Rev.* **116**, 600–621.

Wilson, M. F., Henderson-Sellers, A., Dickinson, R. E. and Kennedy, P. J. 1987. Sensitivity of the biosphere-atmosphere transfer scheme (BATS) to the inclusion of variable soil characteristics. *J. Clim. Appl. Met.* **26**, 341–362.